The Effects of Heat Treatment on the Chromium Depletion, Precipitate Evolution, and Corrosion Resistance of INCONEL Alloy 690

J.J. KAI, G.P. YU, C.H. TSAI, M.N. LIU, and S.C. YAO

A series of heat treatments were performed to study the sensitization and the stress corrosion cracking (SCC) behavior of INCONEL Alloy 690. The microstructural evolution and the chromium depletion near grain boundaries were carefully studied using analytical electron microscopy (AEM). The measured chromium depletion profiles were matched well to the calculated results from a thermodynamic/kinetic model. The constant extension rate test (CERT) was performed in the solution containing 0.001 M sodium thiosulfate ($Na_2S_2O_3$) to study the SCC resistance of this alloy. The Huey test was also performed in a boiling 65 pct HNO_3 solution for 48 hours to study the intergranular attack (IGA) resistance of this alloy. Both tests showed that INCONEL 690 has very good corrosion resistance. It is believed that the superior IGA and SCC resistances of this alloy are due to the high chromium concentration (~30 wt pct). It is concluded in this study that INCONEL 690 may be a better alloy than INCONEL 600 for use as the steam generator (S/G) tubing material for pressurized water reactors (PWR's).

I. INTRODUCTION

INCONEL* Alloy 690 is an austenitic nickel-based alloy which has been proposed as a substitute material for INCONEL Alloy 600 in steam generator (S/G) tubing in PWR's because of its much higher chromium concentration (28 to 31 wt pct *vs* 15 to 17 wt pct). It is well-known that INCONEL 600 suffers IGA and SCC failure if it is used in an aggressive environment. Since 1970, broken tubes in S/G's have become a vital defect for PWR's. From the statistics presented by Tatone,[1] it is found that SCC is becoming the most serious cause for the failure of PWR steam generator tubes. Therefore, it is essential to find a material which has good resistance to SCC.

There are some data indicating that thermally-treated INCONEL 690 is a better corrosion-resistant tubing material than other alloys, such as 304SS, 316SS, INCOLOY* 800, INCONEL 600, *etc.*[2,3] This alloy is immune to SCC in primary water,[4,5,6] all-volatile treated water (AVT) environment,[7] chloride solution,[5,8] and sulfate solution.[8] Although the corrosion behavior of INCONEL 690 has been reported frequently, there is still a lack of a systematic study of the microstructural evolution and the chromium depletion near grain boundaries during heat treatment and the effect of that on the IGA and SCC resistances of INCONEL 690.

This study was aimed to investigate the effect of heat treatment on the chromium depletion and precipitate evolution near grain boundaries of INCONEL 690 and to study the SCC and IGA behaviors of this alloy. The results of this study address the feasibility of substituting INCONEL 600 with a higher chromium alloy, INCONEL 690, to be used as S/G tubing material.

*INCONEL and INCOLOY are trademarks of Inco Alloys International, Inc., Huntington, WV.

J.J. KAI, Associate Professor, G.P. YU, Professor, C.H. TSAI, Professor and Chairman, M.N. LIU, Graduate Student, and S.C. YAO, Graduate Student, are with the Department of Nuclear Engineering, National Tsing Hua University, 101, Section II, Kuang-Fu Road, Hsinchu, Taiwan, Republic of China.

Manuscript submitted November 17, 1988.

II. EXPERIMENTAL PROCEDURES

The plate-type INCONEL Alloy 690 used in this study was supplied by Huntington Alloys, Inc., Huntington, WV. It was received in a mill-annealed (MA) condition, and the chemical composition is given in Table I. Three types of specimens were prepared from the plate for various testing purposes. Specimens of 3-mm-diameter discs were used for scanning transmission electron microscope/energy dispersive spectrometer (STEM/EDS) examinations. Samples of 30 mm × 10 mm × 3 mm size were used for the IGA Huey test. The dimensions of the specimens used in the CERT were the same as those of the tensile test specimens which were described in Reference 12. The specimens were first solution-annealed (SA) at 1150 °C for 1 hour followed by water quenching (WQ) to dissolve all the carbides in the matrix. These specimens were then isothermally treated for various periods of time, respectively:

(1) 538 °C/24, 48, 100, 200 h + WQ;
(2) 600 °C/1, 5, 10, 24, 48, 100, 215 h + WQ;
(3) 700 °C/1, 5, 10, 24, 48, 100 h + WQ; and
(4) 800 °C/1, 10 h + WQ.

The transmission electron microscope (TEM) specimens were prepared by using a twin-jet electropolisher with a polishing solution which consisted of 10 pct $HClO_4$ and 90 pct methanol under the conditions of 600 mA, −20 °C, and 25 cm^3/s flow rate. The microstructural analysis and the precipitate identification were performed using a JEOL-200CX TEM/SCAN electron microscope. The chromium depletion near the grain boundary was studied using an X-ray EDS. The EDS measurement was done near grain boundary areas between two adjacent precipitates and along a straight line

Table I. The Chemical Composition of INCONEL 690 Analyzed by Inductively Coupled Plasma Atomic Emission Spectroscopy (ICP-AES) and High-Temperature Combustion C/S Method

Elements	Ni	Cr	Fe	C	Si	Al	Ti	Cu	S	Nb
Wt pct	bal.	28.57	9.35	0.024	0.3	0.3	0.26	0.1	0.003	0.0007

which is perpendicular to the grain boundary. The electron probe size was about 20 nm in diameter. The spacing between test points varied from 50 to 200 nm. At least two specimens were examined for each annealing condition, and two different grain boundary areas of each specimen were measured to quantify the chemical composition. The quantitative chemical composition analysis was done using the Cliff-Lorimer equation[9] with the original material as a standard. A detailed description of the quantitative analysis was reported elsewhere.[10–13]

In the Huey test, the samples were mechanically polished to 600-grit SiC abrasives. These samples were then boiled in a 65 pct nitric acid (HNO_3) solution, which was contained in a modified Erlenmeyer flask/modified Allihn condenser at 117 °C for 48 hours. The weights of these samples were recorded before and after the test. The sample surfaces were examined with an optical microscope (OM) to study the corrosion type and morphology.

In the CERT, the specimens were mechanically ground to 1200-grit SiC abrasives. These specimens were then tested in an Instron Model 1342 testing machine in 0.001 M $Na_2S_2O_3$ and pH 3 at room temperature with a strain rate of 1×10^{-6} s^{-1}. A load *vs* time curve was recorded for each tested specimen, and the fracture surface was examined using a scanning electron microscope (SEM).

The measured chromium depletion profiles were compared to the results which were calculated based on a thermodynamic/kinetic model. The thermodynamic model was modified from a model developed by Was and Kruger[14] originally for INCONEL 600. The same assumptions were made as stated in Reference 14, except that in INCONEL 690, the carbides were identified as $M_{23}C_6$ instead of M_7C_3 in INCONEL 600. The carbon solubility, which was adopted from Scarberry *et al.*[22] for INCONEL 690, was lower than that used in INCONEL 600. The binary and ternary interaction terms were assumed to be the same as in INCONEL 600. The kinetic process was then controlled by one-dimensional volumetric diffusion of chromium, in which the diffusion coefficients were adjusted to best-fit the measured profiles. This model was also rewritten as a program coded in PASCAL* for execution on an IBM** personal computer.

*PASCAL is a trademark of Oregon Software, Inc., Portland, OR.
**IBM is a trademark of International Business Machines Corporation, Armonk, NY.

III. RESULTS

A. *The Effect of Thermal Treatment*

The average grain size of the INCONEL 690 specimens grew from about 7 μm (in mill-annealed condition) to about 24 μm after solution annealing at 1150 °C for 1 hour. Figures 1(a) and (b) show the optical micrographs of the INCONEL 690 specimens in the MA and SA conditions, respectively. It was also observed that the subsequent thermal treatment had little effect on the grain size of this alloy. Figures 1(c) and (d) show the TEM microstructures of MA and SA specimens, respectively. It was clearly observed that after the solution annealing (1150 °C/1 h + WQ), all the carbides which originally existed in the as-received specimen (MA) were dissolved into the matrix. The effects of the subsequent heat treatments following the solution annealing on the INCONEL 690 specimens were separated into two portions: namely, the effect on the precipitate morphology and that on the chromium depletion along grain boundaries.

1. *The precipitate morphology*

The carbides which were observed in all the INCONEL 690 specimens examined were identified as $M_{23}C_6$ with an fcc crystal structure and a lattice parameter of $a_0 = 1.06$ nm. Figures 2(a) and (b) show the bright-field and dark-field images, respectively, of an $M_{23}C_6$ carbide, which sticks out of the edge of a perforation hole. Figures 2(c) and (d) show the selected area diffraction pattern (SADP) of the $M_{23}C_6$ carbide and the identified spots of this precipitate. In the pictures, the *m* represents matrix and *p* precipitate. It was clearly observed that this type of carbide has a cube-to-cube orientation relationship to the fcc austenitic matrix structure (lattice parameter $a_0 \cong 0.35$ nm). Figure 2(e) shows the EDS analysis of a carbide that sticks out of the edge of a perforation hole. The analysis revealed that all the carbides contained a very high chromium concentration (usually greater than 85 wt pct).

Figures 3, 4, 5, and 6 illustrate the TEM microstructures of the grain boundary precipitates of the INCONEL 690 specimens heat-treated for various time periods at 538 °C, 600 °C, 700 °C, and 800 °C, respectively. It was observed that the precipitate morphology varied dramatically with the thermal treating time and temperature. In general, the precipitate morphologies can be roughly divided into four categories: fine and discrete, fine semicontinuous, large semicontinuous, and coarse and discrete. Table II summarizes the observed results of the precipitate morphology in INCONEL 690. The quantitative summarization of the precipitate size, number density, and average distance between particles is shown in Table III. In some specimens which were heat-treated for a longer period of time (*e.g.*, 538 °C/200 h, 600 °C/100 h, 215 h, 700 °C/48 h, 100 h) or were heated at high temperature (*e.g.*, 800 °C/1 h, 10 h), there were some fine carbides observed in the matrix. These fine carbides were usually formed along a dislocation line (Figures 3(c) and 4(d)) or on the twin boundary (Figures 5(e) and 6(c)) and were also identified as $M_{23}C_6$, just like those found on the grain boundary.

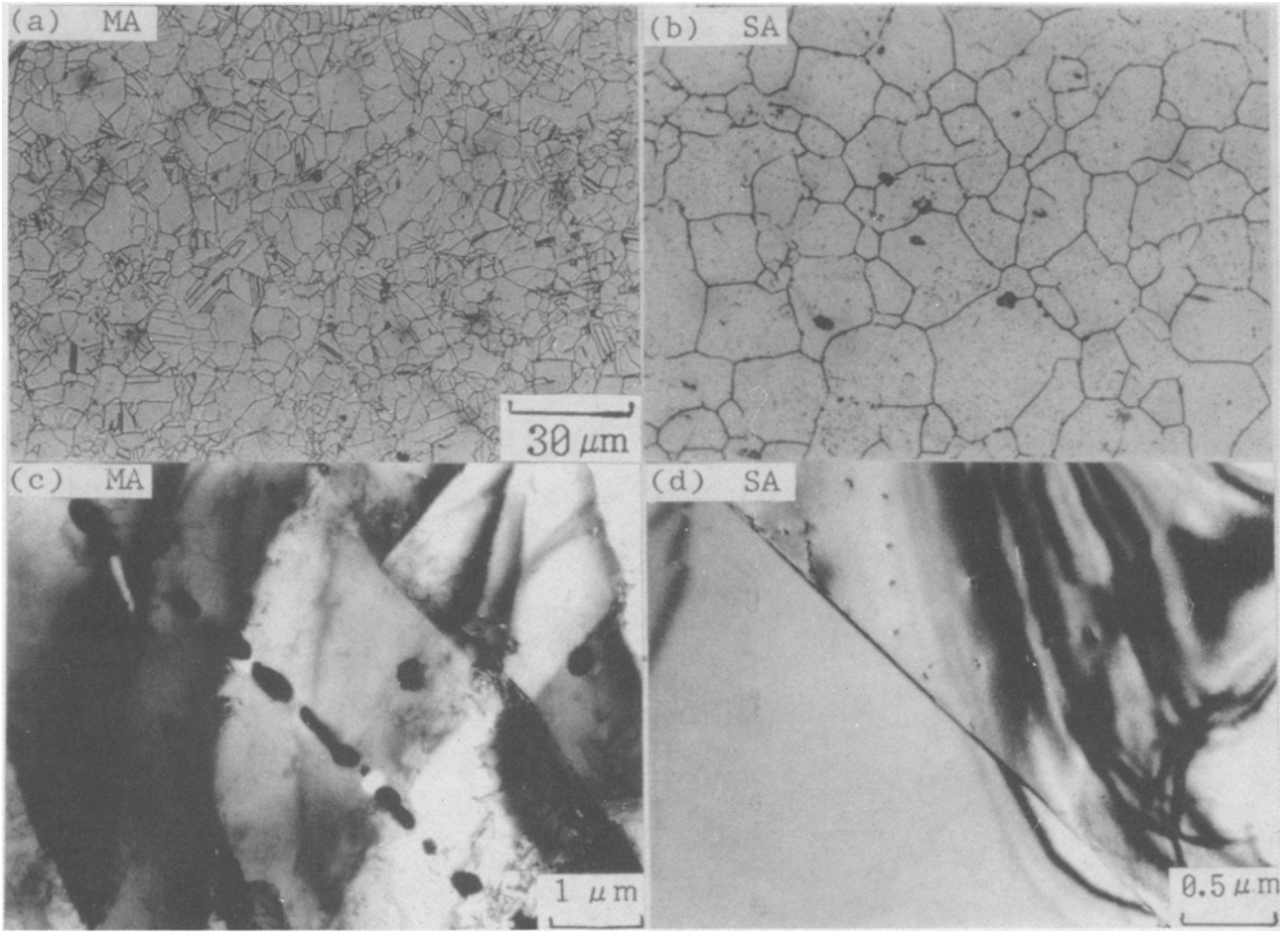

Fig. 1—The ((*a*) and (*b*)) optical ((*c*) and (*d*)) TEM micrographs of the MA and SA specimens.

2. *Chromium depletion at the grain boundary*

The measured chromium depletion profiles near grain boundaries of various heat-treated specimens are shown in Figures 7(a), (b), (c), and (d) for the temperatures of 538 °C, 600 °C, 700 °C, and 800 °C, respectively. The error bars expressed in the measured data included both the statistical uncertainties (such as standard deviation and grain size variation, *etc.*) and the systematic errors (namely, spot size effect, beam broadening, and image drifting, *etc.*).[12,13]

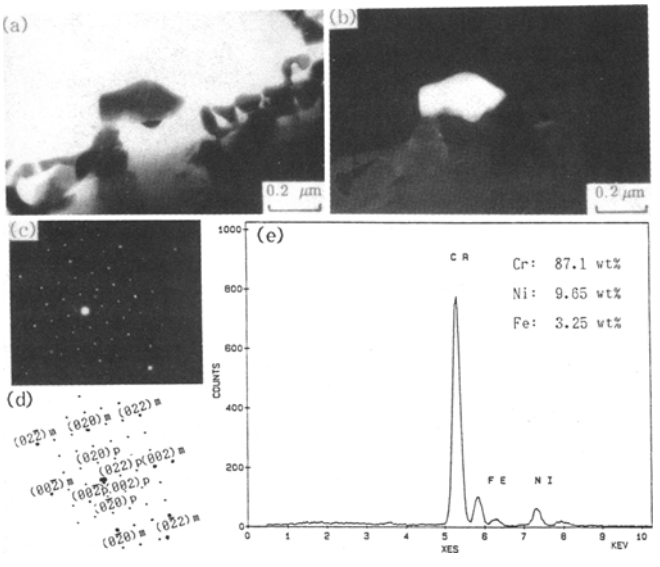

Fig. 2—The identification of the $M_{23}C_6$ precipitate in INCONEL 690. (*a*) Bright-field image, (*b*) dark-field image, (*c*) SADP, (*d*) identification of SADP, and (*e*) EDS analysis.

The chromium concentration at the grain boundary was the lowest value relative to other areas in all the specimens. This chromium concentration at the grain boundary showed first a decrease and then an increase with heating time for the 538 °C, 600 °C, and 700 °C series. In the 800 °C series, the chromium concentration at the grain boundary was increased with increasing time. The full width at half maximum (FWHM) of the chromium depletion profiles always increased with heating time for all four temperatures.

Figure 8 shows a comparison between the measured data and the calculated results from a thermodynamic/kinetic model for the 700 °C series of specimens. It was found that the calculated data matched the experimental results well except in the longer time cases (*e.g.*, 700 °C/48 h, 100 h). In those cases, the specimen was already self-healed, according to the measurement, while the model still predicted a depletion near the grain boundary. This discrepancy will be discussed later.

Table IV summarizes the measured chromium concentration at the grain boundary for all heat-treating conditions. It was observed that the minimum chromium

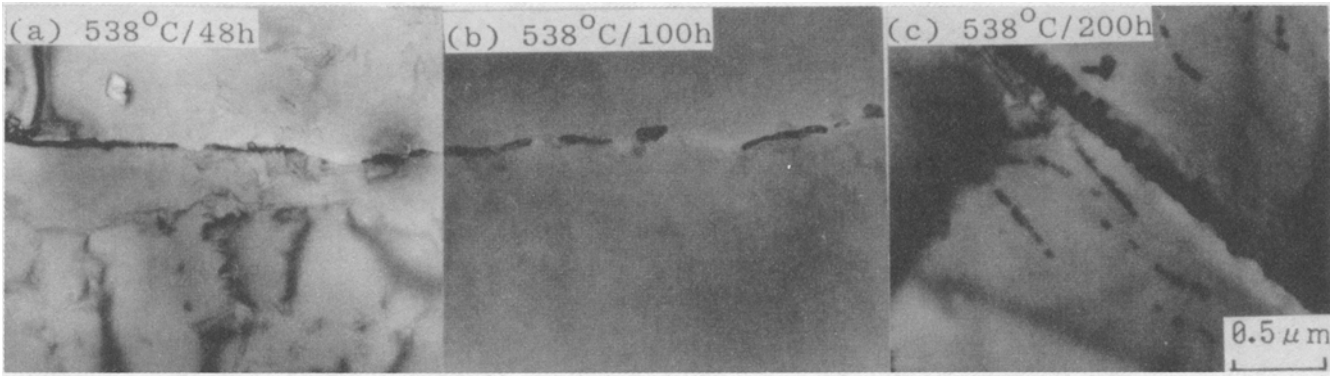

Fig. 3—The TEM microstructures of the INCONEL 690 specimens heat-treated at 538 °C.

concentration reached about 18 wt pct, which occurred in the 538 °C/100 h and 600 °C/48 h cases.

B. *The Huey Test*

Table V illustrates the results of the Huey test. The weight loss of each specimen after 2 days of experiments was too low to distinguish any differences among various heat treatment conditions. The OM micrographs of the surface of the specimens after the Huey test showed a very slight IGA for all the specimens. Therefore, it was concluded that there was no sensitization of INCONEL 690 after heat treating in the temperature range of 538 °C to 800 °C for the periods of time treated in this study.

C. *The Constant Extension Rate Test (CERT)*

The CERT was done on an Instron Model 1342 testing machine in a solution of 0.001 M $Na_2S_2O_3$ and pH 3 at room temperature and with a strain rate of 1×10^{-6} s^{-1}. The ultimate tensile stress and the 0.2 pct yield stress of the INCONEL Alloy 690 were about 620 MPa and 250 MPa, respectively. Figure 9 shows the CERT results for various heat-treating conditions. Figure 10 shows the SEM microstructures of the fracture surfaces of the tested specimens. All specimens tested showed a ductile behavior with an elongation around 70 pct. Table VI summarizes the testing results. The SEM examination showed that the fracture surface consisted of dimples and holes, which indicated that it was a ductile fracture.

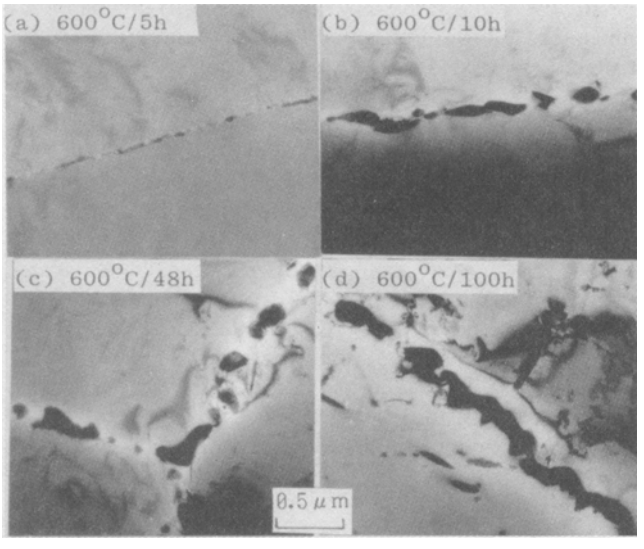

Fig. 4—The TEM microstructures of the INCONEL 690 specimens heat-treated at 600 °C.

IV. DISCUSSION

A. *Precipitate Morphology*

The evolution of precipitate morphology during the heat treatment is a result of a regular thermal diffusion process, as schematically illustrated in Figure 11. After solution annealing at 1150 °C for 1 hour, all the original carbides were dissolved in the matrix, and the alloy became a homogeneous solid solution (Figure 11(a)). During subsequent heat treatments, carbides formed in the grain boundaries, and since carbon atoms diffuse much faster than other alloy elements in the material, carbon activity is assumed to be uniform in the whole matrix, which is determined by the initial carbon content and the rate of carbon consumption. Because chromium atoms are relatively strong carbide formers, carbide formation depressed interfacial chromium concentration (Figure 11(b)) and left a steep chromium concentration gradient. Following carbide formation and chromium depletion, chromium atoms diffused from the matrix to the carbide-matrix interfaces (Figure 11(c)). This thermal diffusion process induced the carbide morphology and chromium depletion profile evolution, which continued until all free carbon atoms were consumed; *i.e.*, the available carbon concentration reached the solubility limit (Figure 11(d)).

B. *The Chromium Depletion Profile*

From the comparison between the measured chromium depletion profiles and the calculated results shown in Figure 8, it was clearly observed that they were matched quite well for the 700 °C series except for the longer periods of time (48 hours and 100 hours). These discrepancies might be explained by the formation of intragranular precipitates in the matrix, which would reduce the amount of available free carbon, thus decreasing the chromium depletion effect along the grain boundary areas.

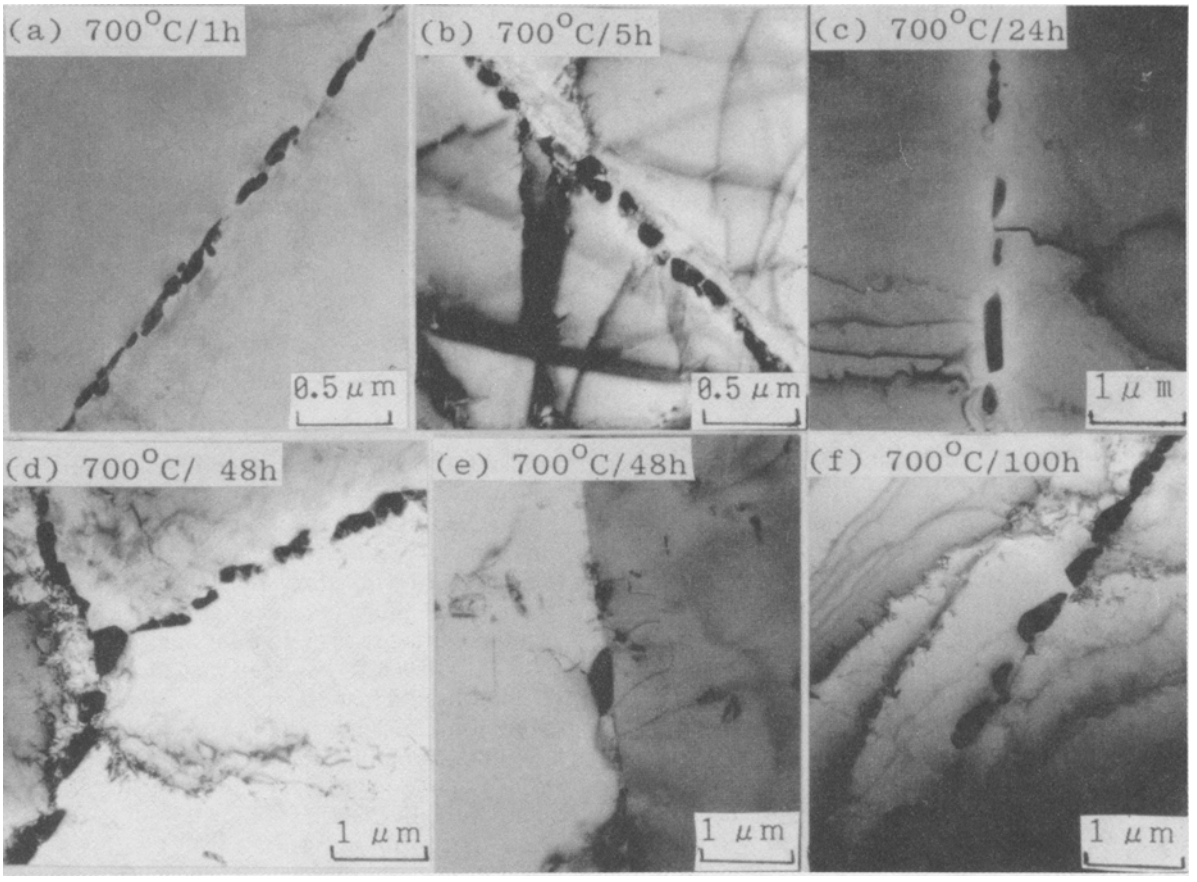

Fig. 5—The TEM microstructures of the INCONEL 690 specimens heat-treated at 700 °C.

Since the thermodynamic/kinetic model did not consider the formation of intragranular precipitates, it was quite reasonable that the calculated value would be lower than that measured by STEM/EDS.

There were also some discrepancies in the equilibrium minimum chromium concentration between the measured results (≥18 wt pct) and the calculated data (≥13 wt pct) in the 538 °C and 600 °C cases. This was explained by two reasons. First, the model assumed that the thermodynamic equilibrium at grain boundary was reached instantaneously,[14,15] which might be hampered by the nucleation kinetics; second, at lower temperatures, the slopes of the chromium concentration profile vary very steeply so that the beam size, image drifting, and beam broadening have larger effects on the measurements.[13,15] Therefore, it was believed that the actual value of the interfacial chromium concentration at the grain boundary in these cases should be less than the measured data but higher than the calculated results.

The measured results showed that the minimum chromium concentration at the grain boundary was a function of heating time. In the 538 °C, 600 °C,

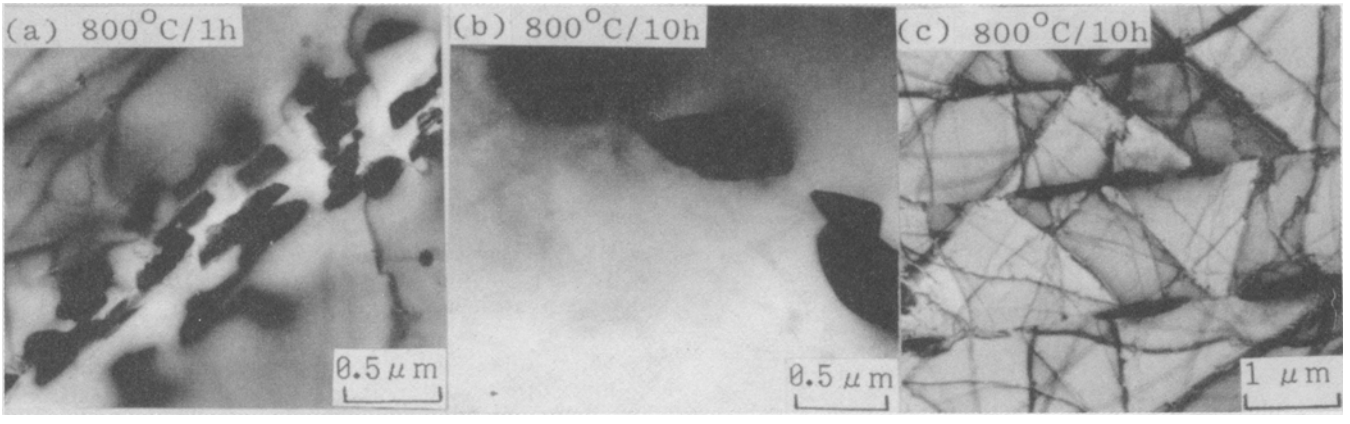

Fig. 6—The TEM microstructures of the INCONEL 690 specimens heat-treated at 800 °C.

Table II. The Carbide Morphology of INCONEL 690 after Various Heat Treatments

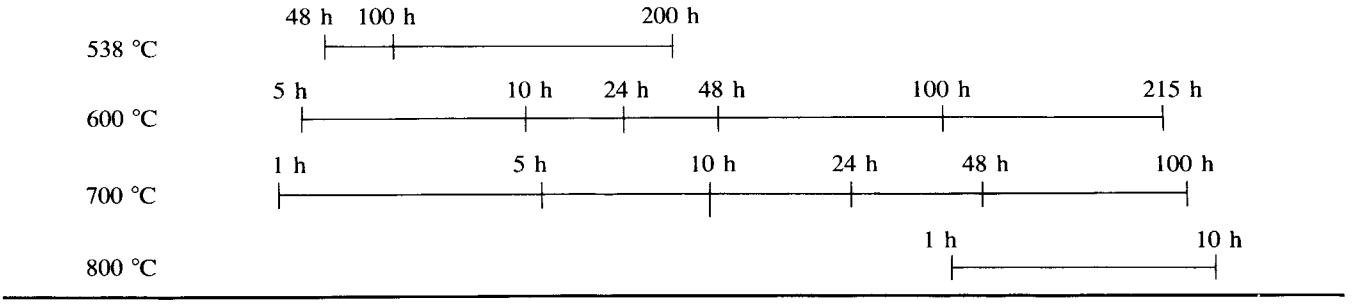

and 700 °C series, the minimum chromium concentration at grain boundary decreased first and then increased with increasing time. However, in the 800 °C series, it increased with increasing time. This result is consistent with the results of INCONEL Alloy 600 studies.[12,13,16,17] The study on stainless steel[18] showed a similar result also. The FWHM of the chromium depletion profile, however, increased with increasing heat-treating time for all temperature series. This trend agreed quite well with the calculated data and the results of INCONEL 600 studies.[13,16,17]

Figure 12(a) shows the effect of grain size on the chromium depletion profile. Three grain sizes were chosen, namely, 10, 30, and 70 μm. It was clearly observed that the variation of grain size has little effect on the 700 °C/1 h case; however, it does have a larger effect on the 700 °C/48 h case. The reason for this is because under the same carbon consumption rate due to the intergranular carbide formation, the carbon concentration in the matrix will decrease faster in a smaller grain than in a larger grain. Therefore, after the same period of heat-treating time, the chromium concentration near the grain boundary area will be higher for a smaller grain. For a shorter period of heating time, the carbon content in the matrix is still relatively high so that there is little difference between the small and large grain. However, after a long period of heating time, the carbon content approached the solubility limit of carbon in the matrix; therefore, it becomes very sensitive to the grain size.

Figure 12(b) illustrates the calculated minimum equilibrium chromium concentration at the grain boundary as a function of temperature for both INCONEL 600 and INCONEL 690. It was seen that the heat-treating temperature has a great effect on the value of the minimum chromium concentration. For example, at 500 °C, the minimum chromium concentration at the grain boundary will decrease to 12.5 wt pct for INCONEL 690 and 6 wt pct for INCONEL 600.

Previous studies on an INCONEL Alloy 600 revealed that under a sulfur-contaminated environment, the critical chromium concentration for resisting SCC failure is around 8 wt pct or 9 to 10 wt pct,[19,21] depending on the test conditions. This study indicated that the minimum chromium concentration at the grain boundary of various heat-treated INCONEL 690 specimens was around 18 wt pct (the measured results) or 13 wt pct (the calculated data) and above. If the SCC failure mechanism of these two alloys is similar to each other, which is quite possible, then it can be concluded that the SCC failure due to a sensitization effect may not occur in the INCONEL Alloy 690.

Table III. The Quantitative Analysis of Precipitate Size, Number Density, and Average Distance between Particles

Heat Treatment	Average Density (No./μm)	Average Length (μm)	Average Distance between Particles (μm)
538 °C/100 h	6.3	0.08	0.078
538 °C/200 h	9.5	0.10	0.005
600 °C/5 h	10.2	0.05	0.046
600 °C/10 h	5.06	0.15	0.049
600 °C/48 h	4.81	0.16	0.048
600 °C/100 h	4.58	0.18	0.039
600 °C/215 h	4.12	0.19	0.053
700 °C/1 h	7.87	0.09	0.036
700 °C/5 h	7.28	0.11	0.03
700 °C/10 h	4.13	0.16	0.082
700 °C/24 h	2.41	0.27	0.142
700 °C/48 h	2.43	0.28	0.132
700 °C/100 h	2.59	0.29	0.093
800 °C/1 h	2.69	0.30	0.073
800 °C/10 h	1.42	0.48	0.223

C. *The Huey Test and the CERT*

The results of the Huey test indicated that the IGA resistance of INCONEL 690 was indeed superior to that of INCONEL 600. Previous study[19] on INCONEL 600 using the modified Huey test (in 40 pct nitric acid solution boiling for 24 hours) showed that the IGA resistance of INCONEL 600 is sensitive to the chromium depletion parameter related to the profile width. The most sensitized heat treatments for INCONEL 600 after solution annealing at 1120 °C for 30 minutes are 800 °C/1 h, 700 °C/3 h, and 600 °C/10 h. On INCONEL 690, however, the results of the modified Huey Test (in 65 pct nitric acid and boiling for 48 hours) showed no significant intergranular corrosion or differences of weight loss between different heat-treated specimens.

The results of the CERT also illustrated that the SCC failure of INCONEL 690 was not observed under the test conditions. All specimens showed a ductility above 70 pct

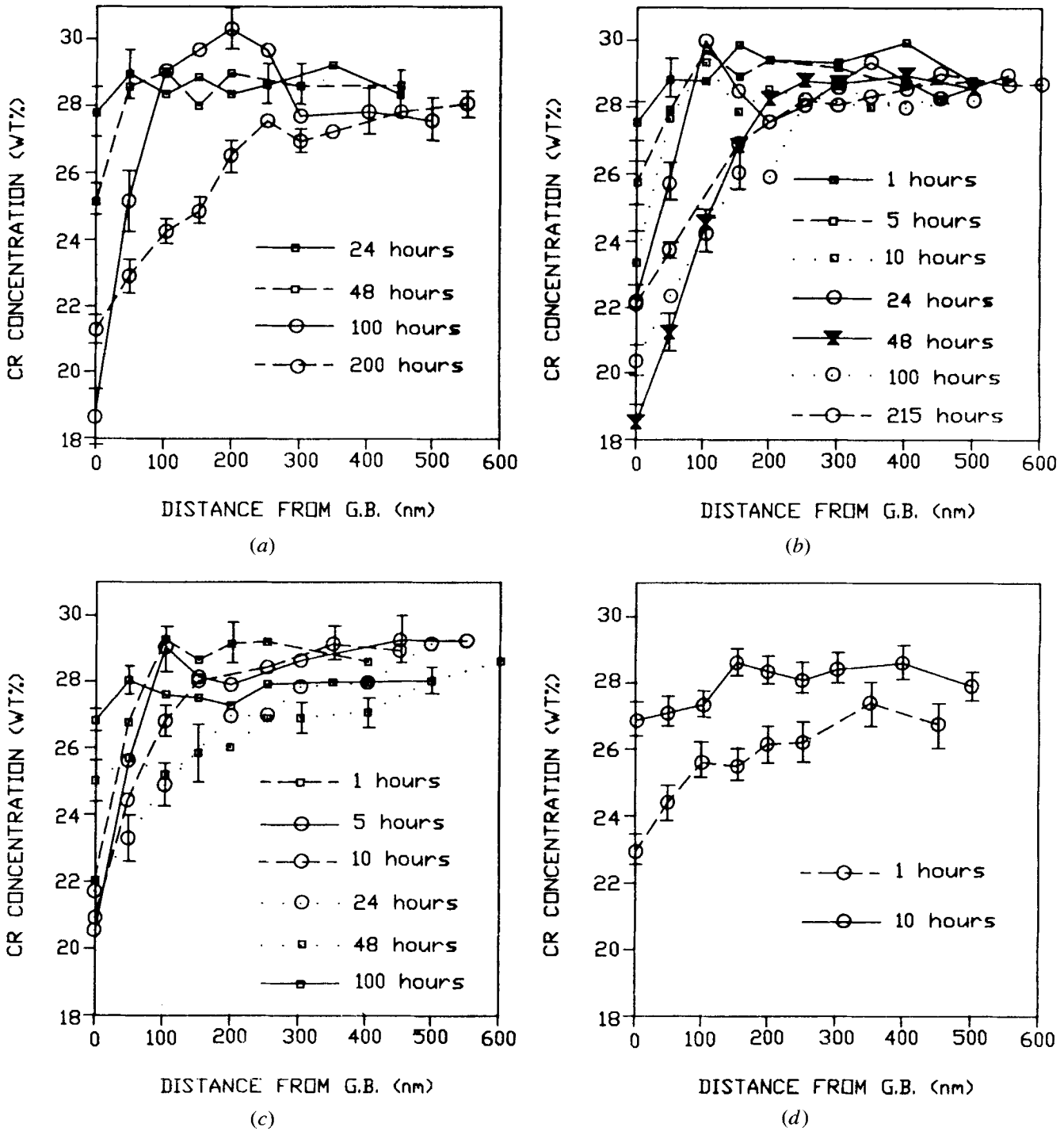

Fig. 7—The chromium depletion profiles near grain boundaries of various heat-treated specimens: (*a*) 538 °C, (*b*) 600 °C, (*c*) 700 °C, and (*d*) 800 °C.

Table IV. The Measured Minimum Chromium Concentration at the Grain Boundary of Various Heat-Treated INCONEL 690 Specimens

	Time (h)						
Temperature (°C)	1	5	10	24	48	100	200
538	—	—	—	27.9	25.2	18.6	21.4
600	27.5	25.7	23.4	22.3	18.5	20.4	22.1
700	22.0	20.5	21.0	21.6	25.0	26.9	—
800	22.9	—	26.8	26.8	—	—	—

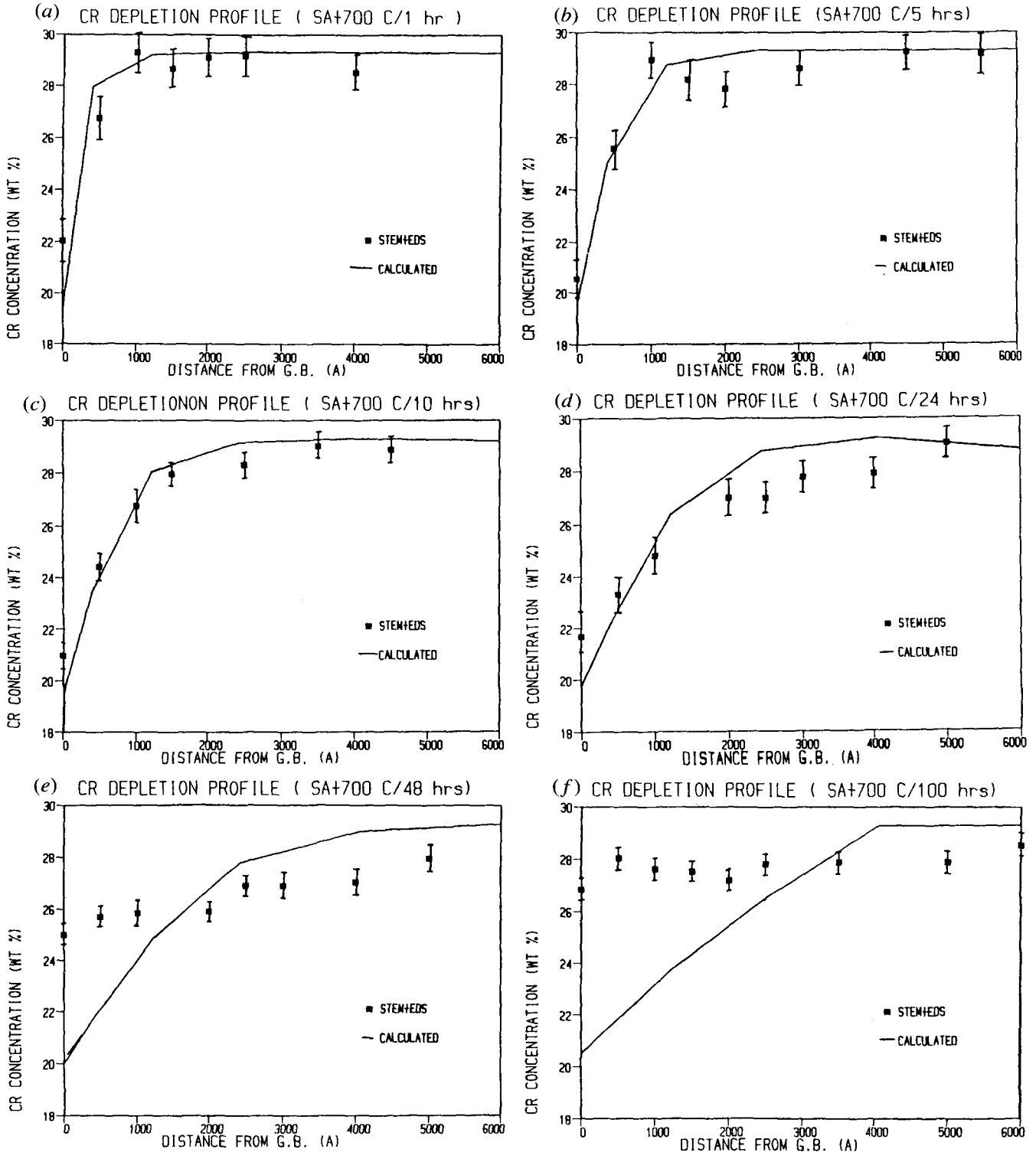

Fig. 8—A comparison between the measured results and the calculated results of the chromium depletion profiles near the grain boundary area of specimens heat-treated at 700 °C.

Table V. The Results of the Huey Test (Weight Loss in mm/yr)

Temperature (°C)	Time (h)							
	0.5	1	5	10	24	48	100	200
538	0.05	0.05	<0.05	0.1	0.1	0.05	0.1	0.1
600	0.1	0.1	<0.05	0.05	0.05	0.05	<0.05	—
700	0.1	0.05	0.1	<0.05	<0.05	0.05	<0.05	—
800	0.1	0.1	0.1	0.1	0.1	0.1	<0.05	—

elongation, and the fracture surface was entirely ductile ruptured. On the other hand, the CERT's and constant load SCC tests of INCONEL 600 in thiosulfate solution[19,20] indicated that the SCC resistance was sensitive to the depletion depth (minimum interfacial chromium concentration). Therefore, INCONEL 690 is also superior to INCONEL 600 in terms of SCC resistance.

Both the Huey test and the CERT confirmed the prediction which was made from the chromium depletion measurements in the previous section. The critical chromium concentration to prevent the SCC failure is around 8 wt pct,[12,16,21] and the severe IGA weight loss is around 9 to 10 wt pct[13,19] for INCONEL 600. Since both the measured minimum chromium concentration at the grain boundary (18 wt pct) and the calculated results (13 wt pct) were much higher than the critical chromium concentra-

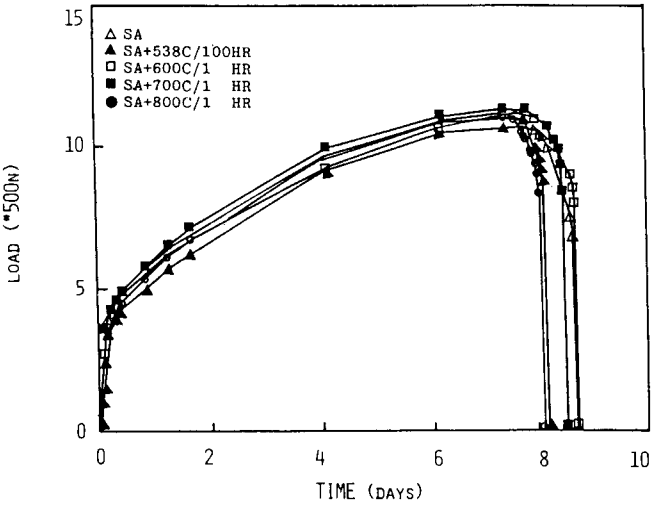

Fig. 9—The stress *vs* strain curves of the INCONEL 690 specimens during the CERT.

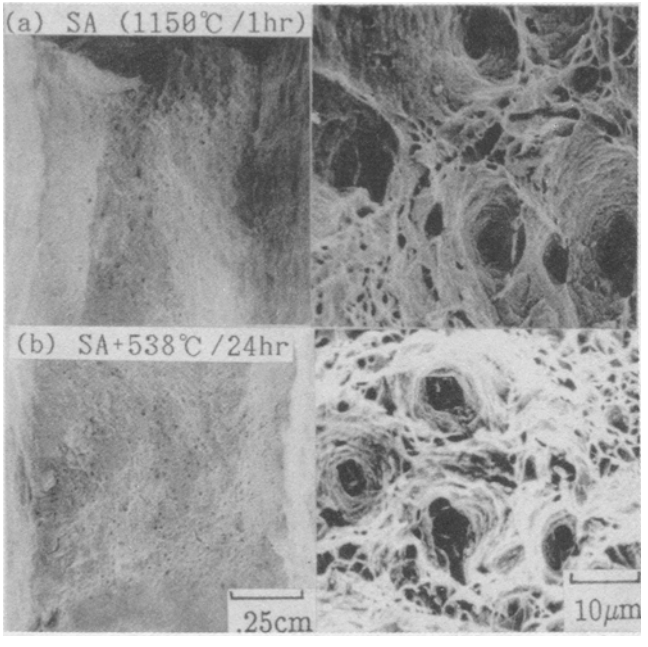

Fig. 10—The SEM microstructures of the fracture surface of the constant extension rate tested specimens.

Table VI. The CERT Results of Various Heat-Treated INCONEL 690 Specimens (pH = 3, 0.001 M $S_2O_3^{-2}$, 1 × 10^{-6} s^{-1})

Heat Treatment	Elongation (pct)	Ultimate Tensile Stress (MPa)
538 °C/24 h	74.9	583
538 °C/48 h	73.9	583
538 °C/100 h	68.4	627
600 °C/1 h	73.9	622
700 °C/1 h	70.4	633
700 °C/3 h	70.4	633
700 °C/5 h	70.5	635
800 °C/1 h	71.2	611
SA	72.9	633

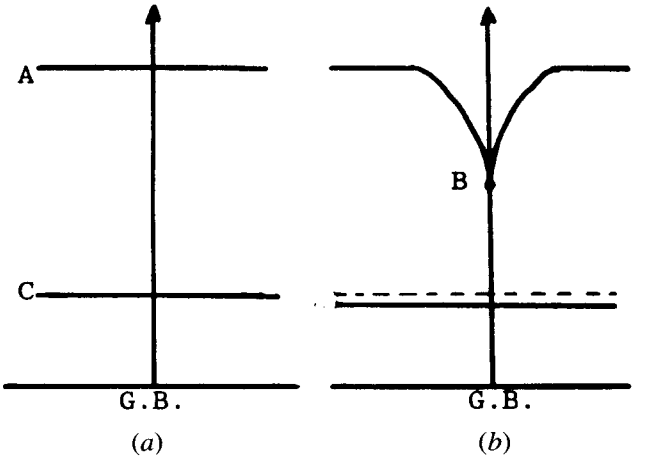

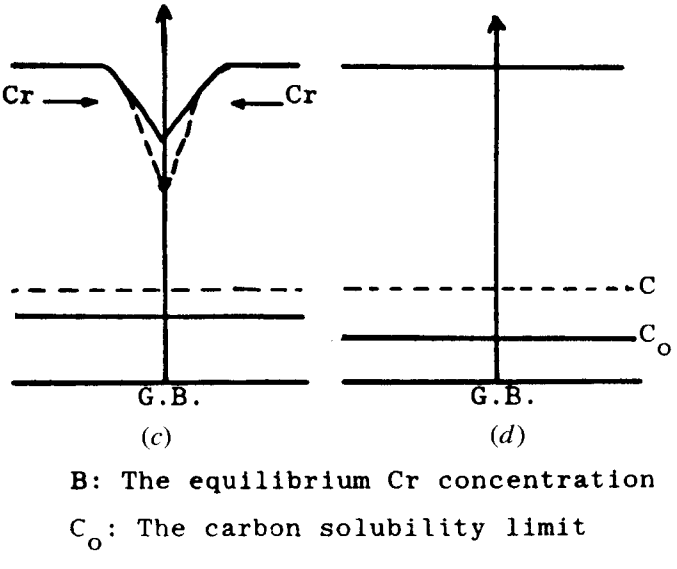

Fig. 11—The schematic diagrams of chromium depletion and carbon consumption around the grain boundary area during heat treatment. (*a*) After SA, the alloy is a homogeneous solid solution; (*b*) during subsequent heating, chromium depletion along grain boundaries due to carbide formation; (*c*) chromium atoms diffuse from matrix to grain boundaries due to concentration gradient; and (*d*) carbon concentration reaches solubility limit and the kinetics cease.

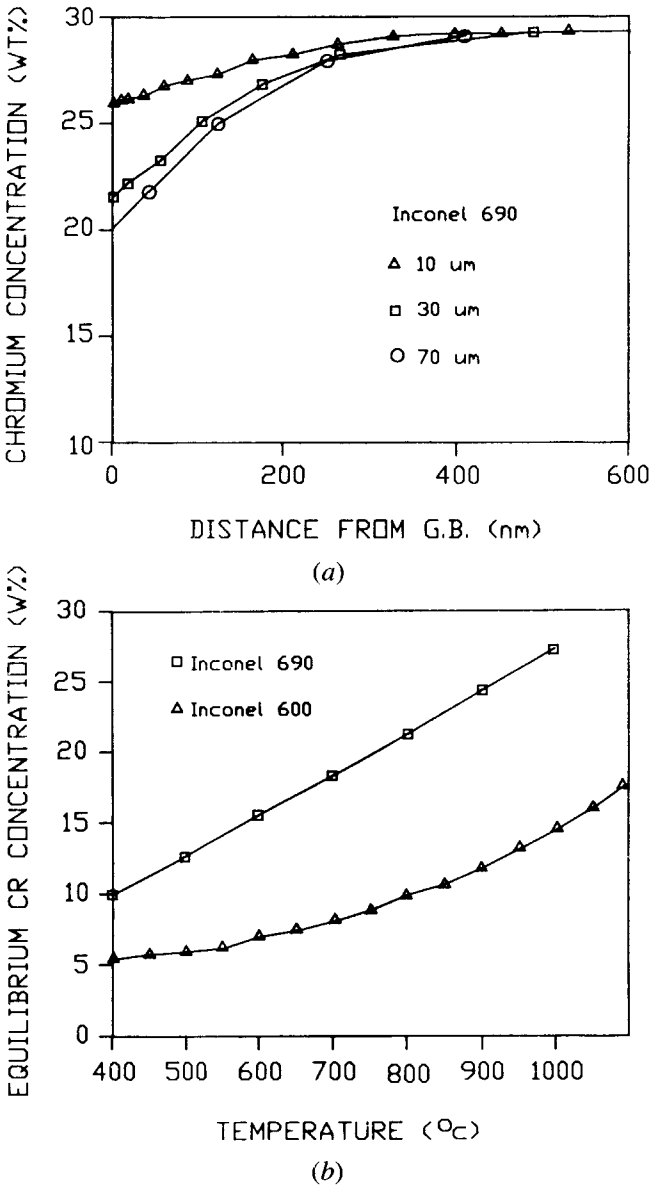

Fig. 12—The effect of (*a*) the grain size and (*b*) the heat-treating temperature on the chromium depletion profile.

tion, it was quite reasonable to conclude that because of the higher paraequilibrium chromium concentration due to the high chromium content of INCONEL 690, the SCC failure caused by a sensitization effect may not occur in this alloy.

V. CONCLUSIONS

1. INCONEL 690 may be a better alloy than INCONEL 600 for use as the S/G tubing material for PWR's due to its higher chromium content and better resistance to IGA and SCC failures.
2. The carbides that were observed in the INCONEL 690 specimens were found to be in the form of $M_{23}C_6$ with an fcc crystal structure (a_0 = 1.06 nm). The metallic composition of this precipitate consisted of mostly chromium (≥85 wt pct) and some iron and nickel. The morphology of carbides is in discrete or semi-continuous forms, depending on the heat-treating temperature and time.
3. The chromium depletion near the grain boundary area of the INCONEL 690 specimens after thermal treatment was studied. The chromium concentration at the grain boundary showed first a decrease and then an increase with increasing time in the 538 °C, 600 °C, and 700 °C series. The FWHM of the chromium depletion profiles increased with time for all four temperatures.
4. The Huey tests demonstrated that the superior IGA resistance of INCONEL 690 was not affected by the heat treatment in the temperature range of 538 °C to 800 °C for a time period of 1 to 200 hours.
5. No SCC failure occurred in the CERT in 0.001 M $Na_2S_2O_3$ and pH 3 at room temperature. All specimens showed ductile rupture mode with a 70 pct elongation or above.
6. The superior IGA and SCC resistances of INCONEL 690 were attributed to its high chromium content, which resulted in the high paraequilibrium chromium concentration at the grain boundary and, therefore, avoided the serious sensitization effect.
7. A thermodynamic/kinetic model was modified in this study to identify the chromium depletion phenomenon in INCONEL 690, and the results were used to compare with the measured data.

ACKNOWLEDGMENTS

The authors would like to thank Ms. L.C. Wang for her assistance in the EDS measurements. This work was financially supported by the National Science Council of the Republic of China under Contract Nos. NSC 77-0413-E007-10 and NSC 77-0413-E007-06.

REFERENCES

1. O.S. Tatone: *Nucl. Eng. Int. (NEL)*, June 1986, pp. 81-83.
2. A.J. Sedricks, J.W. Schultz, and M.A. Cordovi: *Boshoku Gijutsu (Corros. Eng.)*, 1979, vol. 28, pp. 82-95.
3. P.H. Berge and J.R. Donati: *Nucl. Technol.*, 1981, vol. 55, pp. 88-104.
4. G.P. Airey, A.R. Vaia, and R.G. Aspden: *Nucl. Technol.*, 1981, vol. 55, pp. 436-48.
5. T. Yonezawa, K. Onimura, T. Kusakabe, H. Nagano, K. Yamanaka, M. Inoue, N. Sasaguri, and T. Minami: Mitsubishi Heavy Industries, Ltd., and Sumitomo Metal Industries, Ltd., Takasago, Japan, unpublished research, 1985.
6. R.A. Page and A. McMinn: *Metall. Trans. A*, 1986, vol. 17A, pp. 877-87.
7. B.P. Miglin and C.E. Shoemaker: *Corrosion/86*, 1986, paper no. 255.
8. Inconel Alloy 690, Huntington Alloys, Inc., Huntington, WV, 1980.
9. G. Cliff and G.W. Lorimer: *Proc. 5th Europ. Cong. on Electron Microscopy*, Institute of Physics, Bristol, U.K., 1972, p. 140.
10. J.I. Goldstein: in *Introduction to Analytical Electron Microscopy*, J.J. Hren, J.I. Goldstein, and D.C. Joy, eds., Plenum Press, New York, NY, 1979, ch. 3, pp. 83-120.
11. N.J. Zaluzec: in *Introduction to Analytical Electron Microscopy*, J.J. Hren, J.I. Goldstein, and D.C. Joy, eds., Plenum Press, New York, NY, 1979, ch. 4, pp. 121-67.
12. J.J. Kai, C.H. Tsai, T.A. Huang, and M.N. Liu: *Metall. Trans. A*, 1989, vol. 20A, pp. 1077-88.

13. L.H. Wang and T.A. Huang: Department of Nuclear Engineering, National Tsing Hua University, Hsinchu, Taiwan, Republic of China, private communication, 1987.
14. G.S. Was and R.M. Kruger: *Acta Metall.*, 1985, vol. 33 (5), pp. 841-54.
15. S.C. Yao and M.N. Liu: Department of Nuclear Engineering, National Tsing Hua University, Hsinchu, Taiwan, Republic of China, private communication, 1988.
16. G.S. Was, H.H. Tischner, and P.M. Latanision: *Metall. Trans. A*, 1981, vol. 12A, pp. 1397-408.
17. E.L. Hall and C.L. Briant: *Metall. Trans. A*, 1985, vol. 16A, pp. 1225-36.
18. E.L. Hall and C.L. Briant: *Metall. Trans. A*, 1984, vol. 15A, pp. 793-811.
19. C.H. Tsai, J.J. Kai, G.P. Yu, and S.S. Hsu: Department of Nuclear Engineering, National Tsing Hua University, Hsinchu, Taiwan, Republic of China, unpublished research, 1987.
20. V.B. Rajan and G.S. Was: *Corrosion/86*, 1986, paper no. 252.
21. J.J. Kai, C.H. Tsai, and T.A. Huang: *Trans. Am. Nucl. Soc.*, 1988, vol. 56, pp. 247-49.
22. R.C. Scarberry, W. Mankins, and M. Pohovey: EPRI Workshop on Thermally Treated Alloy 690 Tubes for Nuclear Steam Generators, EPRI, Palo Alto, CA, 1985.